Coupling phenomena in superconducting Nb/Fe multilayers

G. Verbanck, C. D. Potter,* V. Metlushko,† R. Schad,‡ V. V. Moshchalkov, and Y. Bruynseraede
Laboratorium voor Vaste-Stoffysica en Magnetisme, Katholieke Universiteit Leuven, Celestijnenlaan 200D, B-3001 Leuven, Belgium
(Received 7 July 1997; revised manuscript received 30 October 1997)

We measured the critical temperature T_c and critical field H_{c2} of molecular-beam epitaxy-grown Nb/Fe multilayers in which the layer thicknesses t_{Fe} and t_{Nb} are systematically varied. For constant t_{Nb} we observe a continuous decrease of T_c with increasing t_{Fe} up to $t_{Fe}=15$ Å. At higher t_{Fe} values a sudden drop of T_c is measured related to the onset of ferromagnetism in the Fe layers. Measurements of the shape and the angular dependence of $H_{c2}(T)$ clearly show that the superconducting Nb layers are already decoupled for $t_{Fe}=12$ Å, magnetization measurements, however show that the Fe layers are ferromagnetic only for $t_{Fe}\geqslant 16$ Å. For constant $t_{Fe}=25$ Å, the observed strong decrease of T_c with decreasing Nb thickness as well as the temperature dependence of H_{c2} are well described by the theoretical model for decoupled superconductor/ferromagnet multilayers. [S0163-1829(98)04110-1]

INTRODUCTION

The interaction between superconductivity (S) and ferromagnetism (F) has been intensively studied during the last decades through the proximity effect in superconductor/ferromagnet (S/F) multilayers. Theoretical investigation by Radovic *et al.*[1] and Buzdin and co-workers,[2] based on the Usadel equations, predicted the existence of the so-called π-phase state in S/F multilayers for specific thicknesses of the F layer, assuming that the S layers are still coupled. In this case the phase difference of the order parameter between two neighboring S layers equals π, and T_c is predicted to oscillate as a function of the thickness t_F of the ferromagnetic layers. Although early experiments on V/Fe (Ref. 3) suggested this oscillatory behavior, a more systematic study of the V/Fe system by Koorevaar *et al.*,[4] and on Nb/Gd triple layers by Strunk *et al.*,[5] showed no evidence for an oscillatory behavior. Finally $T_c(t_F)$ oscillations in Nb/Gd multilayers with wedge-shaped Gd layers were reported by Jiang *et al.*[6] Although the data showed a qualitative agreement with the theory of Radovic *et al.*,[1] no quantitative agreement was obtained.

Recently, Kuboya and Takanaka[7] calculated T_c for S/F multilayers using the formalism developed by Takahashi and Tachiki.[8] For ferromagnetic layers with a sufficiently strong exchange field the existence of a $T_c(t_F)$ minimum, without the appearance of a $T_c(t_F)$ maximum, is predicted. This might explain why several experiments on S/F multilayers failed to observe T_c oscillations. On the other hand, Mühge *et al.*[9,10] recently found a nonmonotonic behavior of T_c in Fe/Nb/Fe trilayers. They attribute the appearance of this T_c oscillation to a changing interaction of the Cooper pairs with the Fe layers when Fe becomes ferromagnetic.

In order to elucidate the importance of the magnetic interlayer on the coupling properties, we investigated the dependence of the superconducting critical parameters T_c, $H_{c2\parallel}(T)$, and $H_{c2\perp}(T)$ on t_{Fe} in Nb/Fe multilayers. Preliminary results have been published in Ref. 11. We did not observe T_c oscillations, but a sudden drop of T_c appears when the Fe layers become ferromagnetic at $t_{Fe}>15$ Å. This steplike feature is attributed to a larger pair breaking effect when the Fe layers change from the nonmagnetic to the ferromagnetic regime with increasing t_{Fe}. We show that for $t_{Fe}=12$ Å the Nb layers are already completely decoupled, although the Fe remains nonmagnetic until $t_{Fe}=16$ Å. In the second part we compare the theory of Radovic *et al.* for the special case of decoupled S/F multilayers[12] with the change of T_c and $H_{c2}(T)$ in multilayers with varying t_{Nb}. The strong decrease of T_c with decreasing t_{Nb} and the critical field curves are all well described by this model.

EXPERIMENT

The Nb/Fe multilayers were prepared in a Riber molecular-beam epitaxy system (base pressure 2×10^{-11} mbar) using electron beam evaporation hearths, which were rate stabilized to within 1% by a homemade feedback control system using Balzers quadrupole mass spectrometers. The Nb and Fe (purity >99.9% and 99.996%) were evaporated at a typical rate of 1 Å/s on MgO(100) substrates held at 150 °C during deposition. The substrates were cleaned *ex situ* by rinsing in isopropyl alcohol and drying in a dry N_2 flow, and *in situ* by annealing at 600 °C during 15 min. The top and bottom layers of the multilayer are Fe, so that the superconducting layers are always sandwiched between Fe. The top Fe layer is capped by 20 Å of Nb to prevent oxidation. The first set of analyzed multilayers has a constant $t_{Nb}=400$ Å, with $2\text{ Å}<t_{Fe}<34$ Å, and 5 Nb/Fe repetitions, indicated as $[\text{Nb}(400\text{ Å})/\text{Fe}(t_{Fe})]_5$. The second set of films consists of multilayers having a constant $t_{Fe}=25$ Å, but with t_{Nb} varying between 250 Å and 670 Å, and 3 Nb/Fe repetitions. The latter set of samples was prepared in one evaporation run, making use of a movable shutter in front of the substrate holder to vary the Nb thickness for the different samples. The set of multilayers having a variable Fe thickness was made in a similar way, by four consecutive runs of 5 or 6 samples, making sure to have an overlap (in the grown Fe thicknesses) of at least one sample from run to run. We did not observe any systematic differences in the structural properties and resistivity values between samples grown in a different run.

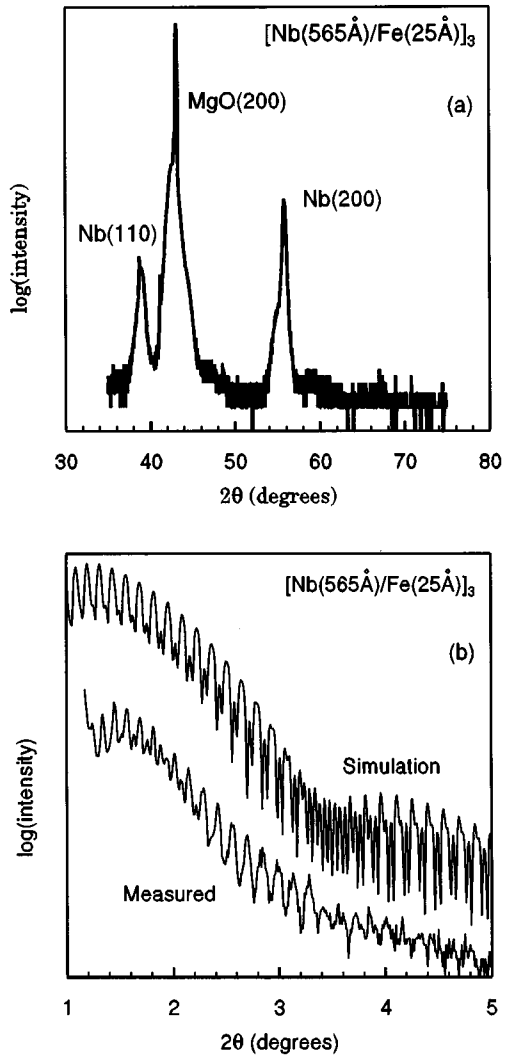

FIG. 1. (a) High-angle diffraction profile of the Nb(565 Å)/Fe(25 Å) multilayer. (b) Measured and simulated low-angle x-ray-diffraction profile of the same multilayer. The simulation is calculated using the SUPREX program (Ref. 12) assuming an interface roughness of 6.5 Å.

The structural characterization was done by both low- and high-angle x-ray-diffraction measurements using a Rigaku rotating anode diffractometer with a wavelength of 1.542 Å (CuK_α). As can be seen in Fig. 1(a) for $[Nb(565\ Å)/Fe(25\ Å)]_3$, the high-angle θ-2θ measurements clearly show the Nb(110) and Nb(200) Bragg reflections at $2\theta = 38.9°$ and 55.75°, respectively. The typical full width at half maximum of the rocking curve of these peaks is 4.0° and 1.0°, respectively. The intensity of the Nb(200) peak is 5 to 10 times larger than the intensity of Nb(110). The material peaks of the Fe could not be observed.

The low-angle-diffraction profiles confirm good layering quality and show that the bilayer thicknesses are within 5% of their nominal values. The final calibration of the thicknesses was based on the low-angle-diffraction results. We have done simulations of the low-angle x-ray profile using the SUPREX program[13] to estimate the roughness at the Nb/Fe interfaces. Figure 1(b) shows the measured and simulated low-angle profile for a $[Nb(565\ Å)/Fe(25\ Å)]_3$ multilayer. For the simulation, an interface roughness of 6.5 Å was used, since this value reproduces best the angle at which the Bragg peaks start to disappear (around $2\theta = 3.4°$). For higher roughness values, the Bragg peaks disappear already at angles smaller than 3°, while for smaller interface roughness the peaks above $2\theta = 3.6°$ are too much pronounced compared to the measured profile. Therefore we conclude from the simulations that the interface roughness is about 6.5 Å.

Magnetic measurements were performed by a superconducting quantum interference device (SQUID) magnetometer enabling to determine the magnetic state of the Fe layers. The superconducting critical parameters T_c, $H_{c2\parallel}(T)$, and $H_{c2\perp}(T)$ were measured resistively using a standard four-probe method in a He^3 Oxford cryostat equipped with a 7 T magnet. The T_c and H_{c2} values were defined as the temperature or the field at the midpoint of the residual normal-state resistance. The 10–90 % transition width at T_c is about 50 mK. For $t_{Nb} = 400$ Å, the resistivity of the multilayers is about 21.5 $\mu\Omega$ cm at room temperature and 4.7 $\mu\Omega$ cm at 10 K, independent of t_{Fe}. For the multilayers with constant t_{Fe}, ρ (300 K) decreases from 19.2 to 16.9 $\mu\Omega$ cm for t_{Nb} changing from 360 to 670 Å, while ρ (10 K) decreases from 2.5 to 1.6 $\mu\Omega$ cm. The value of ρ (10 K) depends on the Nb thickness as $1/t_{Nb}$. The slope of $\rho(1/t_{Nb})$ is too large to explain this behavior by surface scattering according to the Fuchs-Sondheimer theory.[14] These data can however be fitted by the model of Mayadas and Shatzkes[15] for grain-boundary scattering, assuming that the grain size grows with the Nb thickness.

RESULTS AND DISCUSSION

A. Magnetic properties of the Fe layers

Magnetization measurements at $T = 10\ K > T_c$ of $[Nb(400\ Å)/Fe(t_{Fe})]_5$ multilayers show that the Fe layers are not ferromagnetic for $t_{Fe} < 16$ Å. In parallel applied field, a paramagnetic signal is observed when $t_{Fe} \leqslant 14$ Å. The $M(H_\parallel)$ data measured up to 4 T for $t_{Fe} = 6$ Å and $t_{Fe} = 12$ Å show that the magnetization increases linearly at low fields, and is not saturated at 4 T. However, at low temperatures an important contribution to the measured magnetization is caused by magnetic impurities in the MgO substrate. In order to substract the contribution of the substrate, we afterwards removed the multilayer by chemical etching. Substraction of the magnetization of the pure substrate from the initial data, shows that within the experimental error there is no contribution of the Fe layers of that thickness to the magnetization.

For perpendicular fields, the field dependence of the magnetization for the multilayers with $t_{Fe} = 6$ Å and $t_{Fe} = 12$ Å is similar to that for parallel applied field. Therefore, we conclude that for $t_{Fe} < 14$ Å the Fe is nonmagnetic. This might be due to (i) the proximity of the nonmagnetic Nb layers, (ii) the presence of a discontinuous Fe film for very small thicknesses, (iii) the admixture of Fe and Nb at the interfaces leading to the formation of a nonmagnetic FeNb alloy.[16] The latter was observed in Fe/Nb/Fe trilayers by Mühge *et al.*[10] From the value for the roughness at the Nb/Fe interfaces, obtained from simulating the low-angle x-ray spectrum, we

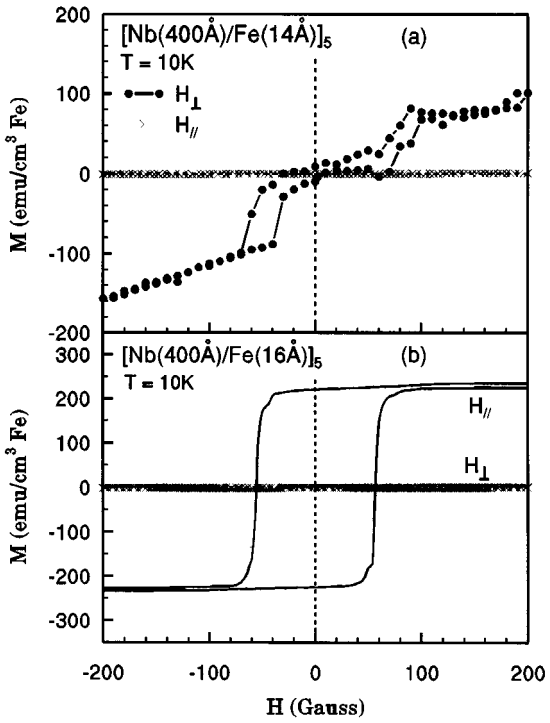

FIG. 2. Magnetization vs applied field measured at $T=10$ K for the samples with $t_{Fe}=14$ Å (a), and $t_{Fe}=16$ Å (b). The data have been corrected for the contribution of the substrate.

conclude that the absence of ferromagnetic order for small Fe thicknesses must primarily be due to alloying effects at the interfaces.

The nonmagnetic behavior of the Fe is most likely related to the formation of resonant *d*-electron states, which are strongly mixed with states in the Nb conduction band. When the width of these resonant states is large enough, the Fe impurity is occupied with both spin-up and spin-down electrons, which leads to the formation of a nonmagnetic state. However, fluctuations at localized spins are still possible: for a short time a magnetic moment might exist due to the time-dependent changes in the occupation numbers for the electrons with spin-up and spin-down.

For $t_{Fe}=14$ Å a jump appears in $M(H_{\perp})$ at approximately ± 70 G [Fig. 2(a)] exhibiting a small hysteresis of about 20 G. However the remanent magnetization is still practically zero. This might indicate a tendency of the Fe magnetic moment to lie perpendicular to the plane of the layers, although no macroscopic ferromagnetism is established yet. This unusual behavior can be attributed to a gradual change from the nonmagnetic to the ferromagnetic regime, since $t_{Fe}=14$ Å is the largest Fe thickness for which no long-range ferromagnetism is observed.

The $M(H)$ curves for $t_{Fe}\geqslant 16$ Å are typical for a ferromagnet with its magnetization in the plane of the film, as shown in Fig. 2(b) for $t_{Fe}=16$ Å. In Fig. 3 we plot the value of the magnetization per unit surface area at $H_{\parallel}=200$ G as function of t_{Fe}. The solid line is the expected result for ferromagnetic Fe having the bulk magnetic moment (2.2 μ_B per atom). From the figure we can see that the saturation magnetization for $t_{Fe}=16$ Å and 34 Å is consistent with the bulk moment of Fe assuming that every Fe layer contains a sub-

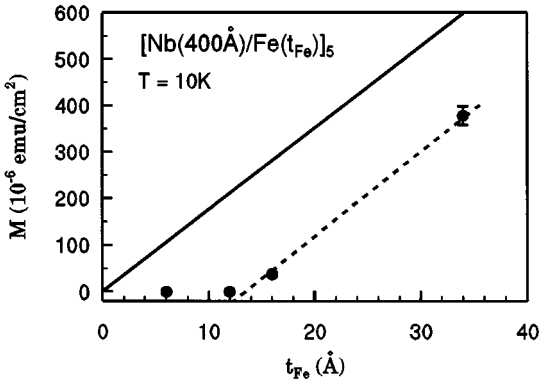

FIG. 3. Magnetization per unit surface area at $H_{\parallel}=200$ G vs Fe thickness for $T=10$ K. The solid line is the expected result for bulk Fe.

layer of about 13 Å that is not contributing to the magnetization. This means that a thin layer corresponding to $t_{Fe}\approx 6.5$ Å at each Nb/Fe interface is magnetically dead, in agreement with the SQUID measurements for $t_{Fe}=12$ Å.

B. Critical temperature and dimensional crossover

Figure 4 shows the critical temperature T_c as function of the Fe thickness for the multilayers with fixed $t_{Nb}=400$ Å. The 10–90 % width of the resistive transition from the normal to the superconducting state is about 45 mK for $t_{Fe}<15$ Å, and 65 mK for $t_{Fe}>19$ Å. For the first two Fe thicknesses which are ferromagnetic, the 10–90 % width of the transition is considerably larger: 630 mK for $t_{Fe}=16$ Å, and 360 mK for $t_{Fe}=20$ Å. This might be due to fluctuations in the Fe thicknesses resulting in different magnetic properties of the Fe at different places.

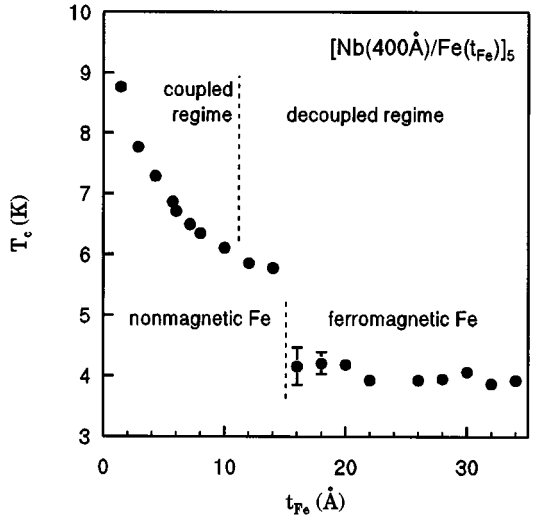

FIG. 4. T_c of Nb/Fe multilayers as function of t_{Fe}. The error bars denote the 10–90 % width of the resistive transition in case it is larger than the symbol size. The onset of the ferromagnetic state of the Fe layers is based on SQUID measurements performed at 10 K. The distinction coupled/decoupled regime is based on the analysis of the critical field data.

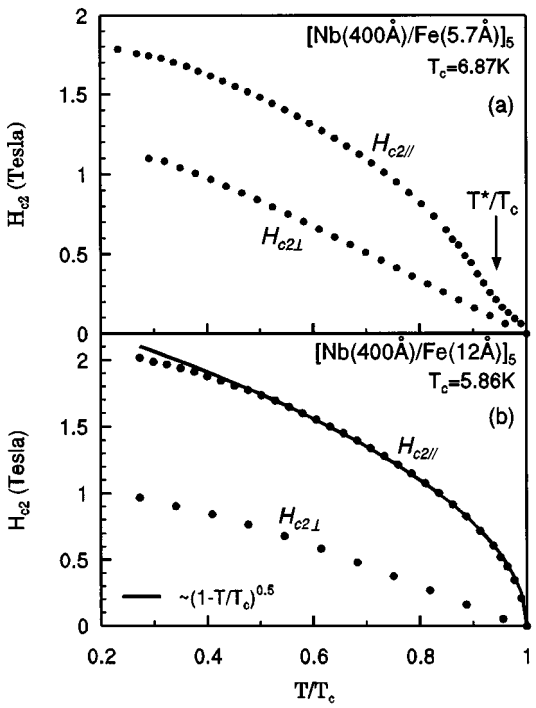

FIG. 5. $H_{c2\parallel}$ and $H_{c2\perp}$ for the multilayers with $t_{Fe}=5.7$ Å (a) and $t_{Fe}=12$ Å (b). The solid line in (b) shows the fitted temperature dependence using Eq. (1).

A smooth decrease of T_c as function of t_{Fe} is observed up to $t_{Fe}=14$ Å. After a sharp drop of T_c at $t_{Fe}\approx 15$ Å, the T_c value becomes independent of the Fe thickness, which is typical for decoupled Nb layers. The drop in T_c cannot be explained due to different sample preparation conditions, since the samples with $8\text{ Å}<t_{Fe}<18$ Å are grown in the same run. The origin of the steplike feature in $T_c(t_{Fe})$ is probably related to the onset of long-range ferromagnetic order in the Fe layers producing a larger pair-breaking effect. A similar step has been observed in Nb/Gd/Nb trilayers when the Gd layer becomes ferromagnetic.[5] We did not observe an increase of T_c for t_{Fe} slightly larger than the value necessary for the onset of ferromagnetism, as recently reported for Fe/Nb/Fe layers.[9]

The strong decrease of T_c for small Fe thicknesses can be explained by the presence of the nonmagnetic Fe resonant states. Experiments by Boato and co-workers[17] showed that nonmagnetic resonant *d* states, formed when Fe-group transition impurities are added into Al, depress the critical temperature much faster than nontransition metal impurities. The origin of this reduced T_c is a weakened attraction of the electrons in a Cooper pair. When such a pair is scattered by a resonant level, the paired electrons, having opposite spins, feel a strong repulsion due to the Coulomb interaction.[18]

To determine at which Fe film thickness the superconducting sheets become decoupled, we measured the upper critical field $H_{c2}(T)$ as shown in Fig. 5. A typical example of the upper critical field curves for the samples in the regime where the superconducting layers are not completely decoupled, is shown in Fig. 5(a) for $t_{Fe}=5.7$ Å. At the temperature T^*, indicated by the arrow in the figure, there is an upturn of $H_{c2\parallel}(T)$. A similar upturn was observed in all the samples with $t_{Fe}\leqslant 10$ Å. T^* gradually approaches the critical temperature as t_{Fe} increases, coinciding with T_c for $t_{Fe}>10$ Å. By using the Ginzburg-Landau (GL) formulas for anisotropic superconductors we can determine the perpendicular and parallel coherence length $\xi_\perp(T)$ and $\xi_\parallel(T)$ and hence the dimensionality. At T^* and for $t_{Fe}=5.7$ Å we find $\xi_\perp(T^*)=280$ Å and $\xi_\parallel(T^*)=640$ Å. For $T>T^*$, $\xi_\perp(T)$ becomes soon larger than the thickness of an individual Nb layer ($=400$ Å), showing that the Nb layers are coupled. Since in this region $\xi_\parallel(T)$ is smaller than or comparable to the total thickness (≈ 2000 Å), the behavior is three-dimensional (3D) as can be seen from the linear dependence of $H_{c2\parallel}(T)$. At lower temperatures, $T<T^*$, $\xi_\perp<t_{Nb}$ and the Nb layers become decoupled, leading to 2D behavior due to the limited Nb thickness.

The crossover temperatures T^* can be well reproduced assuming that the crossover appears when $\xi_\perp(T)$ becomes equal to a fixed thickness $t_{cr}=301$ Å for all the multilayers that are coupled close to T_c. The value for t_{cr} is very close to the effective superconducting thickness of the Nb layers, which equals 310 Å or about $\frac{3}{4}$ of the real Nb thickness, as deduced from the samples in the decoupled regime.

In contrast to the multilayers with $t_{Fe}\leqslant 10$ Å, the observed temperature dependence of $H_{c2\parallel}$ for $t_{Fe}=12$ Å [Fig. 5(b)] is well described by the relation valid for a 2D film in a parallel field [the solid line in Fig. 5(b)],

$$H_{c2\parallel}(T)=H_{c2\parallel}(0)(1-T/T_c)^{1/2}. \quad (1)$$

The good agreement between theory and experiment up to T_c is a clear sign that the Nb layers are decoupled, since the total sample thickness (about 2000 Å) is too large to have 2D behavior over the whole temperature range if the superconducting layers were not decoupled. Moreover the angular dependence of H_{c2} is also correctly described by the Tinkham formula for an individual thin film[19] throughout the whole temperature range,[11]

$$H_{c2}(\theta)|\sin(\theta)|/H_{c2\perp}+[H_{c2}(\theta)\cos(\theta)/H_{c2\parallel}]^2=1. \quad (2)$$

The value $t_{Fe}=12$ Å is substantially smaller than the typical thickness needed to decouple the S layers in superconductor/insulator multilayers, which is about 30–50 Å.[20]

In the decoupled regime, $H_{c2\parallel}(0)$ and $H_{c2\perp}(0)$ should be independent of the Fe thickness. Indeed, for the multilayers with ferromagnetic Fe layers with $16\text{ Å}\leqslant t_{Fe}\leqslant 34$ Å, a maximum difference of 10% was found in $H_{c2}(0)$, showing no systematic dependence on t_{Fe}. We would also like to remark that for $t_{Fe}\geqslant 12$ Å the effective superconducting thickness of the Nb layers, determined from the critical fields, is for the samples both in the ferromagnetic and the nonmagnetic regimes equal to 310 Å. This value is substantially smaller than the real $t_{Nb}=400$ Å, proving that the suppression of the superconducting order parameter does not start at the Nb/Fe interface but well inside the Nb layers.

C. Critical temperature and field in the decoupled regime

In order to investigate the influence of the Nb thickness on the superconducting properties of the multilayer in the decoupled regime, we measured T_c and $H_{c2}(T)$ for structures with a constant $t_{Fe}=25$ Å and varying t_{Nb}. As shown

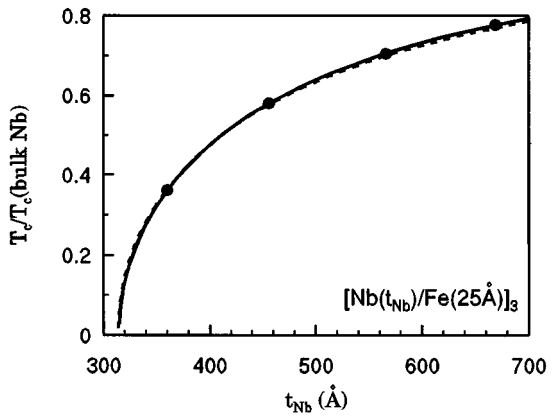

FIG. 6. The normalized critical temperature T_c/T_c(bulk Nb) vs t_{Nb} for decoupled Nb/Fe multilayers. As explained in the text, the dashed line is a one parameter fit to the theory of Ref. 12 using $\varepsilon = 3.77$ and taking $\xi_S = 82.0$ Å as for a 2000-Å-thick single Nb film. The solid line is a two-parameter fit resulting in $\varepsilon = 3.36$ and $\xi_S = 77.76$ Å.

in Fig. 6, T_c decreases rapidly with decreasing Nb thickness. For the sample with the largest Nb thickness, the critical temperature is still considerably lower than for bulk Nb, although the thickness is much larger than $\xi(0)$ ($=130$ Å for bulk Nb, as determined from a 2000 Å-thick single Nb film). For comparison, a single Nb film of 300 Å thickness has a $T_c = 8.7$ K.

The reduction of T_c with decreasing t_{Nb} is well described by the model for decoupled S/F multilayers developed by Radovic *et al.*[12] In the framework of this model the critical temperature is given by

$$\ln(T_c/T_{c0}) = \psi(\tfrac{1}{2}) - \mathrm{Re}\ \psi(\tfrac{1}{2} + \rho^* T_{c0}/T_c), \tag{3}$$

where ψ is the digamma function and T_{c0} the bulk critical temperature. The pair-breaking parameter ρ^* at T_c can be calculated using Usadel's equations for the pair amplitude F_{S} in the superconductor. As a result it is found that ρ^* is determined by the following set of equations:

$$\varphi_0 \tan(\varphi_0) = (1+i)\ \frac{t_{\mathrm{Nb}}/\xi_S}{\varepsilon},$$

$$\varphi_0 = \left.\frac{k_s t_{\mathrm{Nb}}}{2}\right|_{T=T_c},$$

$$k_s^2 = 2\rho^*/\xi_s^2. \tag{4}$$

This means that T_c depends on t_{Nb}, the coherence length ξ_{S} [that is related to the GL coherence length by $\xi_{\mathrm{S}} = 2\xi_{\mathrm{GL}}(0)/\pi$] and the material parameter $\varepsilon = \xi_{\mathrm{F}}/\eta\xi_{\mathrm{S}}$. Here ξ_{F} is the penetration depth of the Cooper pairs into the ferromagnet and η has its origin in the generalized de Gennes-Werthamer boundary condition that has to be fulfilled at the S/F interface for F_{S} and F_{F}, the pair amplitude in the S and F layer, respectively:

$$\frac{\partial}{\partial x} \ln F_{\mathrm{S}} = \eta\ \frac{\partial}{\partial x} \ln F_{\mathrm{F}}. \tag{5}$$

In the dirty limit for specular scattering, $\eta = \sigma_{\mathrm{F}}/\sigma_{\mathrm{S}}$, the ratio of the normal-state conductivities.

The parallel and perpendicular upper critical fields can then be calculated in a similar way by introducing a proper modification of ρ^*. For a perpendicular applied field

$$\rho^* = \rho^*(T_c) + \frac{\pi H_{c2\perp}}{\phi_0}\ \xi_s^2. \tag{6}$$

In the presence of a parallel applied field, the assumption is made that the individual S layers are thin enough, so that the nucleation of superconductivity starts in the middle of the film. In this case the equation for the pair-breaking parameter in a parallel applied field becomes

$$\rho^* = \rho^*(T_c) + \frac{g(\varphi_0)}{24\phi_0^2}\ (2\pi H_{c2\parallel} t_{\mathrm{Nb}} \xi_s)^2, \tag{7}$$

with g a function that is only dependent on φ_0. We remark that for the calculation of the critical fields *no additional parameters* are introduced.

To fit the $T_c(t_{\mathrm{Nb}})$ data to the model of Radovic, using Eqs. (3) and (4), there is in principle only one free parameter ε, since T_{c0} and ξ_{S} can be obtained in an independent way from a thick single Nb film. For a 2000 Å Nb film we found $T_{c0} = 9.15$ K and $\xi_{\mathrm{S}} = 82$ Å. Using these results, the best fit to the measured critical temperatures yields $\varepsilon = 3.77$, the dashed line in Fig. 6. Since there are no free parameters anymore the critical fields can now be calculated. The obtained values for $H_{c2\perp}$ and $H_{c2\parallel}$ are however systematically lower than the measured ones.

To get a better agreement between the model and the data, we therefore used ε and ξ_{S} as fit parameters, but still keeping $T_{c0} = 9.15$ K. The solid line in Fig. 6, which is the best fit to the measured critical temperatures, was obtained by using $\varepsilon = 3.36$ and $\xi_{\mathrm{S}} = 77.8$ Å, a value which is not far off from the previously mentioned 82 Å for Nb. This value for ξ_{S} is also the same as the one reported by Strunk *et al.*[5] for Nb/Gd trilayers and multilayers. There is a very good agreement between $T_c(t_{\mathrm{Nb}})$ and the model, with the two-parameter fit describing the experimental data slightly better. By extrapolating both fits to $T_c = 0$ we see that the critical thickness for superconductivity is about 315 Å, explaining why a multilayer with $t_{\mathrm{Nb}} = 250$ Å did not become superconducting.

In Figs. 7 and 8 we compare our data for, respectively, $H_{c2\perp}(T)$ and $H_{c2\parallel}(T)$ with the model calculations using Eqs. (6) and (7), and using the result of the two-parameter fit to $T_c(t_{\mathrm{Nb}})$, i.e., $\varepsilon = 3.36$ and $\xi_{\mathrm{S}} = 77.8$ Å. There is a good agreement between the model (dashed or solid lines) and the experimental data points, especially for $t_{\mathrm{Nb}} = 360$ Å and $t_{\mathrm{Nb}} = 456$ Å. The deviations in $H_{c2\parallel}(T)$ for $t_{\mathrm{Nb}} \geqslant 566$ Å at low temperatures are due to a crossover of the Nb layers from 2D to 3D behavior. This crossover, appearing when vortex nucleation takes place, cannot be reproduced by the model since the S layers were assumed to be 2D.

An attempt to fit T_c and H_{c2} using for the different multilayers the value ξ_{S} based on the resistivity values failed. In this approach ξ_{S} was determined from the BCS GL-coherence length[21] taking for the electron mean-free path l the values obtained from the product $\rho_{10\,\mathrm{K}} l = 3.75 \times 10^{-16}\ \Omega\mathrm{m}^2$ for Nb.[22] It was however impossible to fit

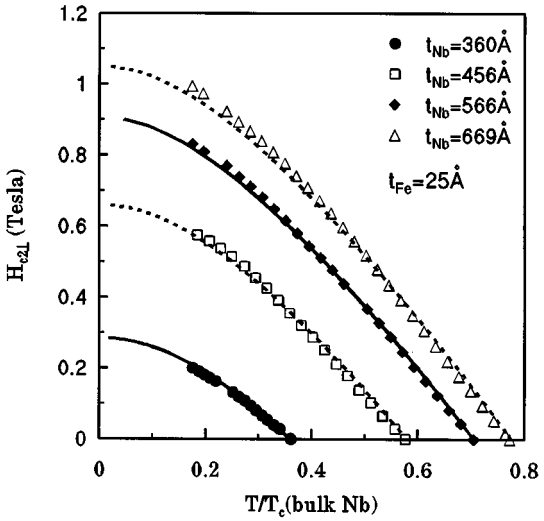

FIG. 7. $H_{c2\perp}(T)$ for the same samples as in Fig. 5. The lines are the model calculations using $\varepsilon = 3.36$ and $\xi_S = 77.76$ Å as explained in the text.

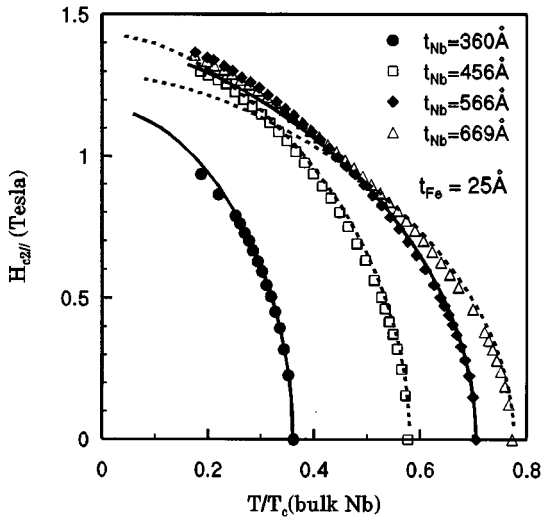

FIG. 8. $H_{c2\parallel}(T)$ for the samples of Fig. 5. The lines are the model calculations using $\varepsilon = 3.36$ and $\xi_S = 77.76$ Å.

$T_c(t_{Fe})$ using a constant ε value. An ε value, varying with thickness, did not allow to fit the observed critical fields.

From the obtained value for ε we can make an estimate of the interface parameter η. Since a Fe layer of 12 Å completely decouples the Nb layers, ξ_F must be of the order of 6 Å, assuming that the decay of superconductivity into the Fe layers starts at the S/F interface. From the equation $\eta = \xi_F/\varepsilon\xi_S$ we then find that η should be about 0.023. Whether this value is plausible can be checked from the resistivities for Fe and Nb. The measured residual resistivity for a 400-Å-thick single Nb film equals $\rho_{Nb} = 2.7\ \mu\Omega$ cm. The value $\eta = 0.023$ then implies $\rho_{Fe} = 115\ \mu\Omega$ cm. This value is not unreasonable, since the resistivity at 4.2 K of a single Fe film of 20 Å, covered with SrF_2 to prevent oxidation, was found to be 30 $\mu\Omega$ cm.

CONCLUSIONS

We studied the superconducting and magnetic properties of Nb/Fe multilayers grown on MgO(001). We have shown that the superconducting Nb layers become decoupled by Fe layers of only 12 Å thickness. Magnetization measurements revealed that for this thickness the Fe layers are still not ferromagnetic. Long-range ferromagnetism occurs only for $t_{Fe} > 15$ Å, resulting in a steplike drop of $T_c(t_{Fe})$ at this thickness. Since we did not observe T_c oscillations vs t_{Fe} a superconducting π-phase state is not present in our multilayers. This is due to the nonmagnetic behavior of the Fe layers for small t_{Fe} and the decoupling of the Nb layers when the Fe is ferromagnetic. Finally we showed that both T_c and H_{c2} as a function of Nb thickness are very well described by the theory of Radovic *et al.* for the decoupled multilayers.

ACKNOWLEDGMENTS

This research was supported by the Fund for Scientific Research Flanders (FWO), the Concerted Research Action programmes (GOA), the Interuniversity Poles of Attraction programs (IUAP)-Belgian State, Prime Minister's Office-Federal Office for Scientific, Technical and Cultural Affairs.

*Present address: Recording Head Group, Seagate Technology, 7801 Computer Ave., South Bloomington, MN.

†Present address: Materials Science Division, Argonne National Laboratory, Argonne, IL 60439.

‡Present address: Research Institute for Materials, K. U. Nijmegen, Toernooiveld 1, NL-6525 ED Nijmegen, The Netherlands.

[1] Z. Radovic, L. Dobrosavljevic-Grujic, A. I. Buzdin, and J. R. Clem, Phys. Rev. B **44**, 759 (1991).

[2] A. I. Buzdin, B. Vujicic, and M. Yu. Kupriyanov, Zh. Eksp. Teor. Fiz. **101**, 231 (1992) [Sov. Phys. JETP **74**, 124 (1992)].

[3] H. K. Wong, B. Y. Jin, H. Q. Yang, J. B. Ketterson, and J. E. Hilliard, J. Low Temp. Phys. **63**, 307 (1986).

[4] P. Koorevaar, Y. Suzuki, R. Coehoorn, and J. Aarts, Phys. Rev. B **49**, 441 (1994).

[5] C. Strunk, C. Sürgers, U. Paschen, and H. v. Löhneysen, Phys. Rev. B **49**, 4053 (1994).

[6] J. S. Jiang, D. Davidovic, D. H. Reich, and C. L. Chien, Phys. Rev. Lett. **74**, 314 (1995).

[7] K. Kuboya and K. Takanaka, Czech. J. Phys. **46**, S2,583 (1996).

[8] S. Takahashi and M. Tachiki, Phys. Rev. B **33**, 4620 (1986).

[9] Th. Mühge, N. N. Garif'yanov, Yu. V. Goryunov, G. G. Khaliullin, L. R. Tagirov, K. Westerholt, I. A. Garifullin, and H. Zabel, Phys. Rev. Lett. **77**, 1857 (1996).

[10] Th. Mühge, K. Westerholt, H. Zabel, N. N. Garif'yanov, Yu. V. Goryunov, I. A. Garifullin, and G. G. Khaliullin, Phys. Rev. B **55**, 8945 (1997).

[11] G. Verbanck, C. D. Potter, R. Schad, P. Belien, V. V. Moshchalkov, and Y. Bruynseraede, Physica C **235-240**, 3295 (1994).

[12] Z. Radovic, L. Dobrosavljevic-Grujic, A. I. Buzdin, and J. R. Clem, Phys. Rev. B **38**, 2388 (1988).

[13] E. E. Fullerton, I. K. Schuller, H. Vanderstraeten, and Y. Bruynseraede, Phys. Rev. B **45**, 9292 (1992).

[14] E. H. Sondheimer, Adv. Phys. **1**, 1 (1952).
[15] A. F. Mayadas and M. Shatzkes, Phys. Rev. B **1**, 1382 (1970).
[16] *Binary Alloy Phase Diagrams*, edited by T. B. Massalski (ASM International, Ohio, 1990), Vol. 2, p. 1732.
[17] G. Boato, G. Gallinaro, and C. Rizzuto, Phys. Rev. **148**, 353 (1966).
[18] C. F. Ratto and A. Blandin, Phys. Rev. **156**, 513 (1967).
[19] M. Tinkham, Phys. Rev. **129**, 2413 (1963).
[20] B. Y. Yin and J. B. Ketterson, Adv. Phys. **38**, 189 (1989).
[21] T. P. Orlando, E. J. McNiff, S. Foner, and M. R. Beasly, Phys. Rev. B **19**, 4545 (1979).
[22] H. W. Weber, E. Seidl, C. Laa, E. Schachinger, M. Prohammer, A. Junod, and D. Eckert, Phys. Rev. B **44**, 7585 (1991).